

# Iron, cobalt or nickel substituted MCM-41 molecular sieves for oxidation of hydrocarbons

V. Parvulescu<sup>1</sup>, B.-L. Su\*

*Laboratoire de Chimie des Matériaux Inorganiques, ISIS, The University of Namur (FUNDP), 61 rue de Bruxelles, B-50 Namur, Belgium*

## Abstract

A series of mesoporous Fe-MCM-41, Co-MCM-41 and Ni-MCM-41 catalysts with different quantity of the metal incorporated in the framework were synthesized and characterized (as-synthesized samples and those after reaction) by X-ray diffraction pattern (XRD), N<sub>2</sub> adsorption–desorption, transmission electron microscopy (TEM), scanning electron microscopy (SEM) and Fourier transform infrared spectroscopy (FTIR) techniques. The effect of the incorporated metal on the MCM-41 surface hydroxyl groups has been evidenced. The catalytic activity and selectivity of these catalysts in liquid phase oxidation of 1-hexene, styrene and benzene with hydrogen peroxide were studied. The structure and morphology of the catalysts before and after reaction were also compared. The results show a high activity and selectivity of catalysts having higher Co content to benzaldehyde from styrene or phenol from benzene, and a low activity of all prepared catalysts in the oxidation of the 1-hexene. The activity and efficiency of H<sub>2</sub>O<sub>2</sub> increases with the metal content and depend on the reaction parameters such as temperature, molar ratio of the reactants and the solvent, and the nature of the reactor. © 2001 Elsevier Science B.V. All rights reserved.

**Keywords:** Iron; Cobalt; Nickel; MCM-41; Benzene adsorption; Hydrocarbon oxidation; Hydrogen peroxide

## 1. Introduction

Hexagonal mesoporous materials, such as MCM-41, offer new opportunities for transition-metal incorporation into silica framework. Owing to their high surface area and high pore volume. It is possible to obtain highly dispersed and isolated active sites in silica framework. In addition, MCM-41 molecular sieves contain a large number of silanol groups at the surface of their channels therefore, a wide variety of reactive metal species can be anchored on the surface by reaction with the silanol groups. Transition metals such as

Ti, V, Mn, Fe, Co, Cr, Mo were introduced in mesoporous MCM-41 molecular sieves by direct synthesis [1–6], impregnation [2,4,7] or complexation (Fe, Cu, Mn) on organofunctionalized Si-MCM-41 [8]. The obtained materials have remarkable catalytic and photocatalytic properties. Recently, serious effort has been devoted to studying the catalytic properties of these so-called redox molecular sieves in the liquid phase oxidation of organic compounds [8,9]. This high interest reflects the need for large pore catalysts to convert bulky molecules in the production of fine chemicals.

The preparation of Co [5,7,10], Fe [8,11,12] and Ni [13] -containing mesoporous molecular sieves by different methods has already been described. However, the catalytic properties and their correlation with the structure have not been studied. Here we will present the preparation, characterization and in particular, the catalytic properties in the oxidation

\* Corresponding author. Tel.: +32-81-724531;  
fax: +32-81-725414.

E-mail address: bao-lian.su@fundp.ac.be (B.-L. Su).

<sup>1</sup>On leave from Institute of Physical Chemistry “I.G. Murgulescu”, Spl. Independentei 202, Bucharest, Romania.

of 1-hexene, styrene and benzene with hydrogen peroxide of well-ordered mesoporous Fe-MCM-41, Co-MCM-41 and Ni-MCM-41 catalysts. Effects of the reaction conditions on the MCM-41 structure and morphology will also be analyzed.

## 2. Experimental

### 2.1. Catalyst preparation

The reagents used for preparing the catalysts were sodium silicate (25.5–28.5% silica, Merck), cetyltrimethylammonium bromide (CTMAB, Aldrich), tetramethylammonium hydroxide (TMAOH solution 25 wt.% in water, Aldrich),  $\text{FeCl}_3$  (Fluka),  $\text{FeSO}_4 \cdot 5\text{H}_2\text{O}$  (Merck),  $\text{Co}(\text{NO}_3)_2 \cdot \text{H}_2\text{O}$  (Merck),  $\text{Ni}(\text{CH}_3\text{COO})_2 \cdot 4\text{H}_2\text{O}$  (Fluka), NaOH and  $\text{H}_2\text{SO}_4$  (Aldrich).

Fe-MCM-41, Co-MCM-41 and Ni-MCM-41 were synthesized by hydrothermal treatment using gel molar composition of  $1.0\text{SiO}_2:x\text{M}^{n+}:0.48\text{CTMAB}:0.28\text{Na}_2\text{O}:3.7\text{TMAOH}:196\text{H}_2\text{O}$  ( $x = 0$  for pure siliceous MCM-41,  $x = 0.02$  and  $0.04$  for  $\text{M} = \text{Fe}, \text{Ni}$  and  $x = 0.02 - 0.1$  for  $\text{M} = \text{Co}$ ). Fe1-MCM-41 and Fe3-MCM-41 have the same composition, but the iron source was different ( $\text{FeSO}_4 \cdot 5\text{H}_2\text{O}$  for Fe1-MCM-41 and  $\text{FeCl}_3$  for Fe3-MCM-41). Fe2-MCM-41 was also prepared with  $\text{FeSO}_4$ , but with  $x = 0.04$ .

Typically, the corresponding quantity of the metal salt in aqueous solution was added to a mixture of 3.8 g sodium silicate, 2.8 g CTMAB and 30 g  $\text{H}_2\text{O}$  under stirring. After 2 h of stirring, 21.7 g TMAOH solution was added. The pH value of the gel was adjusted to 11 with  $\text{H}_2\text{SO}_4$ . The gel obtained was sealed into Teflon-lined steel autoclaves and heated 5 days at 373 K. The solid products were recovered by filtration, washed and dried in air. The as-synthesized samples were calcined at 773 K in a flow of  $\text{N}_2$  followed by air.

The second preparation method utilized for Co-MCM-41 catalyst was impregnation. The catalyst with 1.2 wt.% cobalt was obtained by impregnation of the MCM-41 powder with a solution of cobalt azotate in tetrahydrofuran. The slurry was stirred and refluxed for 3 h at 343 K. The solid was filtered, washed with tetrahydrofuran to remove the cobalt azotate in excess at room temperature, then dried and calcined at 773 K in air.

### 2.2. Characterization

The obtained materials were characterized by X-ray diffraction (XRD) (Philips PW 170 diffractometer),  $\text{N}_2$  adsorption–desorption (Tristar, Micromeritics), Fourier transform infrared spectroscopy (FTIR) (Spectrum 2000, Perkin Elmer), scanning electron microscopy (SEM) (Philips XL-20 microscope) and transmission electron microscopy (TEM) (Tecnai Philips microscope) with an accelerating voltage of 100 kV.

### 2.3. Benzene and ammonia adsorption

The self-supported wafers of calcined samples were loaded in an IR cell and pretreated under oxygen and then under vacuum. A known amount of single compound (benzene or ammonia) was introduced at room temperature until the saturation of the sample wafer. The spectra of adsorbed samples were recorded after each addition of adsorbate (ammonia or benzene). The samples were then heated successively at 323, 373 and 473 K under vacuum for 6 h to remove adsorbed phases.

### 2.4. Catalytic reactions

The catalytic oxidation reactions of 1-hexene, styrene and benzene were performed using 25 cm<sup>3</sup> glass flasks or Teflon lined autoclaves with magnetic stirring for 12–48 h in a temperature range 203–343 K using an oil bath. A total amount of 12 g of reagent, solvent, and oxidant with a molar ratio of hydrocarbons/solvent/ $\text{H}_2\text{O}_2$  (30%) = 1/3.6/3 for 1-hexene and styrene or 1/–/3 for benzene and 70 mg of the catalyst were used. The solvent used for oxidation of 1-hexene and styrene was acetonitrile and all the reactions with benzene were performed without solvent. After reactions, the catalysts were separated by centrifugation and the oxidation products were analyzed using a Carlo Erba gas chromatograph with a 3.5 m stainless steel column (i.d. 3 mm) containing OV-101 coupled with a FID detector. The amount of remaining unreacted  $\text{H}_2\text{O}_2$  was quantified by conventional iodometry. The used catalysts after drying were reutilized for 2 or 3 times in the reaction. The filtrates were resubmitted to reaction conditions to verify the occurrence of leaching of the metal ions.

Table 1  
Characteristics of the obtained mesoporous materials after calcination

Sample	Me content (wt.%)	$d_{100}$ (nm)	$a_0$ (nm)	$S_{\text{BET}}$ (m <sup>2</sup> /g)	$\phi_{\text{BJH}}$ (nm)	Pore volume (cm <sup>3</sup> /g)	Wall thickness (nm) <sup>a</sup>
Si-MCM-41	0	3.75	4.33	1123	2.65	0.810	1.68
Fe1-MCM-41	1.6	3.85	4.45	713	2.50	0.509	1.95
Fe2-MCM-41	3.2	3.89	4.49	689	2.45	0.527	1.94
Fe3-MCM-41	1.6	3.92	4.53	708	2.60	0.562	1.93
Ni1-MCM-41	1.8	3.97	4.58	945	2.85	0.673	1.73
Ni2-MCM-41	3.6	4.01	4.63	915	2.80	0.678	1.83
Co1-MCM-41	1.8	3.99	4.61	990	2.80	0.743	1.81
Co2-MCM-41	3.6	4.09	4.72	905	2.70	0.642	2.02
Co3-MCM-41	5.5	4.11	4.75	644	2.65	0.431	2.10
Co4-MCM-41	7.3	4.17	4.82	568	2.60	0.401	2.22
Co5-MCM-41	9.2	3.92	4.53	681	2.50	0.481	2.03
Co-MCM-41 (i)	1.2 (i)	4.12	4.76	815	2.75	0.667	2.01

<sup>a</sup> Wall thickness ( $w_t$ ) =  $a_0 - \phi_{\text{BJH}}$  [14].

The reutilization of the used catalysts and verification of the reaction activity of filtrates can give some clear idea on catalyst leaching.

### 3. Results and discussion

The amount of metals (Fe, Ni and Co) incorporated in the samples are listed in Table 1. The XRD patterns of calcined Co, Ni and Fe incorporated samples show four sharp diffraction lines (Fig. 1) characteristic of mesoporous materials with hexagonal arrangement of their cylindrical channels. This indicates that all the prepared catalysts have a structure comparable to that

of Si-MCM-41 [14]. Though the silica is stable in the organic solvent, the structure of MCM-41 silica was modified after the impregnation of cobalt azo-tate in tetrahydrofuran since Co-MCM-41 prepared by impregnation method gives a less well-resolved XRD pattern. The XRD patterns of Fe-MCM-41 and Co-MCM-41 samples with Co content higher than 3.6% are also less well resolved. The resolution of XRD patterns decreases with increasing Co content.

The  $d_{100}$  values, unit cell parameter ( $a_0$ ), BET surface area and pore size of all the catalysts are listed in Table 1. The lattice parameters ( $a_0 = 2(3^{1/2})d_{100}$ ) of M-MCM-41 are greater than that of Si-MCM-41. This is consistent with the Me–O bonds being longer than that of Si–O and gives an evidence of the metal incorporation into the framework. It is observed also that the lattice parameters increase with the metal content (except Co5-MCM-41). This indicates that the metal content incorporated in the framework increases with increasing amount of metal salt added in the synthesis gel. However, the decrease in  $a_0$  value from Co4-MCM-41 to Co5-MCM-41 suggests that not all Co amount introduced in the gel are incorporated in the framework of mesostructures.

All the isotherms (Fig. 2) exhibit a sharp inflection at a relative pressure of about 0.36, characteristic of capillary condensation in uniform mesopores. The pore volume and relative pressure of the inflection decrease for the iron sample and when the cobalt content increases. The BJH pore size distribution indicates a narrow and monomodal pore size distribution centered

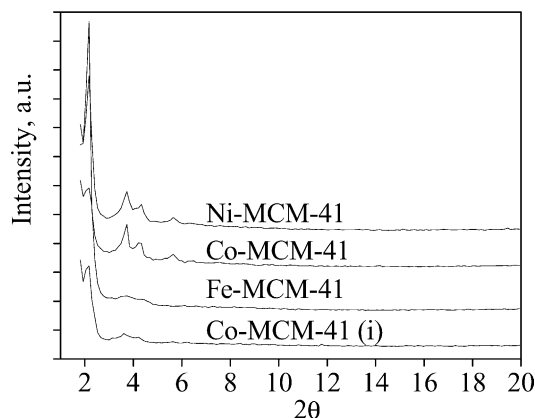


Fig. 1. XRD patterns of the Fe-, Ni- and Co-MCM-41 with different metal contents.

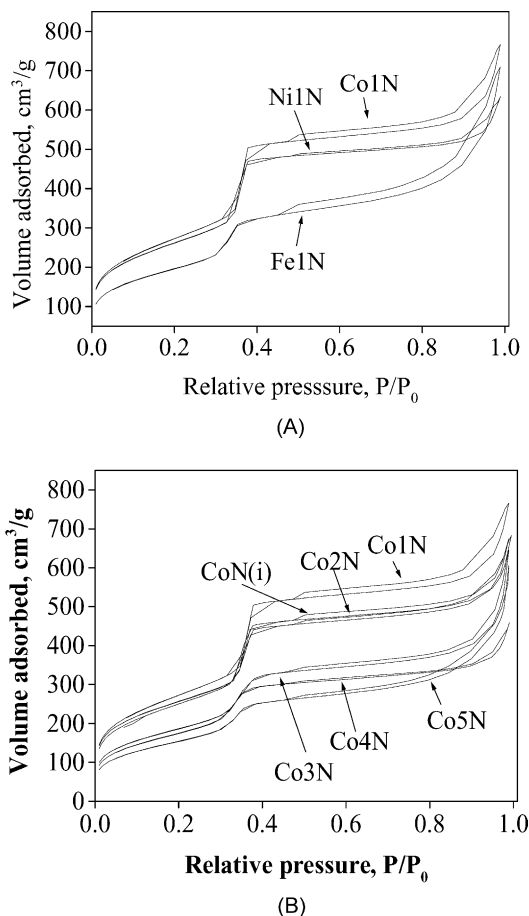


Fig. 2. N<sub>2</sub> adsorption-desorption isotherms of Fe-, Ni- and Co-MCM-41 (A) and Co-MCM-41 with different metal contents (B).

at around  $2.9 \pm 0.2$  nm for all the samples (Table 1). Compared with the Si-MCM-41 sample, the surface area of Me-MCM-41 samples decreases slightly. The high BET surface area, narrow pore size distribution (Table 1) and N<sub>2</sub> isotherms confirm the uniform mesoporosity and organized structure of our materials.

The ordered structure with hexagonal arrangement of channels of our materials was further confirmed by TEM (Figs. 3 and 4A). SEM micrographs show that Ni-MCM-41 catalyst after calcination (Fig. 5) have a morphology of agglomerates of very small spheres.

The IR spectra (not shown here) of the calcined Si-MCM-41 and MeSi-MCM-41 samples show no observable and apparent effect of the cation incorporation on the surface characteristics (same intensity and

same wavenumber of silanols). A sharp intense silanol group is observed at  $3740\text{ cm}^{-1}$ . After introduction of ammonia, this sharp peak is shifted toward lower wavenumber due to the interactions of ammonia with silanol groups and the shift extent can be used to evaluate the acid strength of the silanol groups [15–18]. The shift extent of all metal incorporated samples is similar ( $\Delta\nu = 720\text{ cm}^{-1}$ ) and lower than that of pure siliceous MCM-41 ( $\Delta\nu = 770\text{ cm}^{-1}$ ). This is another proof of substitution of Si by metal atoms in the framework and also indicates that the substitution of Si atoms by transition metal atoms can modify and weaken the acidity of silanol groups. Upon adsorption of benzene, the sharp peak of silanols is also shifted towards low wavenumber (at around  $3600\text{ cm}^{-1}$ ). The incorporation of metal ions in the framework induces, furthermore, a modification in adsorption capacity of ammonia and benzene. The benzene sorption of Si-MCM-41, Fe1-MCM-41, Co1-MCM-41, Co5-MCM-41 and Ni1-MCM-41 expressed by absorbency of peak located at around  $3600\text{ cm}^{-1}$ , arising from the interaction of benzene and silanol groups, as a function of benzene loading is presented in Fig. 6.

The benzene adsorption capacity ranks in the order: Si-MCM-41  $\approx$  Fe1-MCM-41 > Co1-MCM-41 > Ni1-MCM-41 > Co5-MCM-41. The vibration bands (not shown here) of ammonia and benzene adsorbed on the surface indicate a large distribution of the acid sites. They are assigned to Brönsted acid sites (structural or due to surface hydroxyl groups) and Lewis acid sites arising from coordinated metal in the framework. The presence of the Fe(III) in the framework can generate strong Brönsted acid sites and weak Lewis acid sites. The adsorption capacity of iron-containing samples is similar to that of Si-MCM-41, despite its lower surface area (Fig. 6, Table 1).

The reaction conditions and results for oxidation of styrene, benzene and 1-hexene with aqueous H<sub>2</sub>O<sub>2</sub> (30%) are presented in Table 2. It can be seen that Co1-MCM-41 catalyst (with 1.8 wt.% cobalt) and Co-MCM-41 prepared by impregnation has very low activity compared to that of Fe1-MCM-41 and Ni1-MCM-41. However, the activity and efficiency of the H<sub>2</sub>O<sub>2</sub> (H<sub>2</sub>O<sub>2</sub> quantity used for oxidation/H<sub>2</sub>O<sub>2</sub> quantity transformed) of Co-incorporated catalysts prepared by direct synthesis increases sharply with metal content. A high selectivity (80–96%) for the benzaldehyde (oxidation of styrene) or the phenol

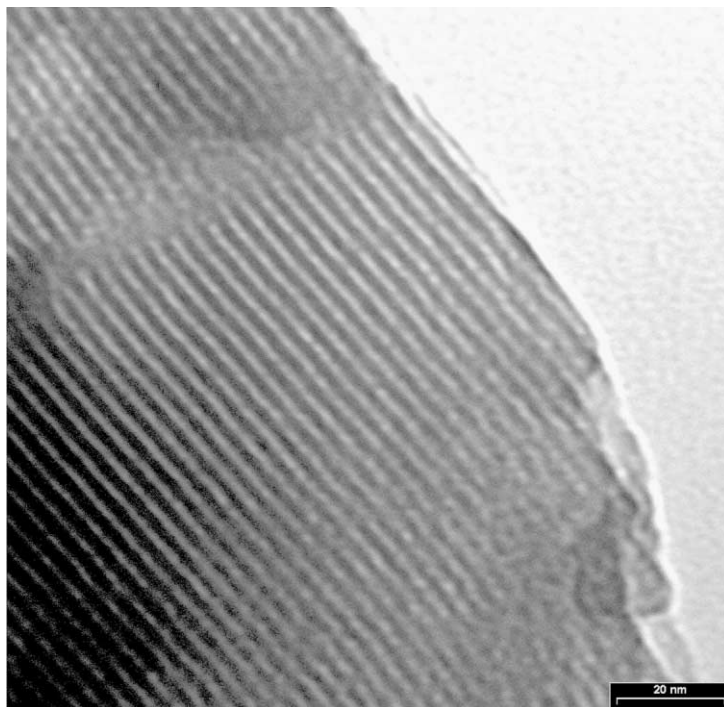


Fig. 3. TEM of as-synthesized Ni-MCM-41 material after calcination.

(oxidation of benzene) is obtained. It is true that the low activity of the impregnated Co-MCM-41 catalyst is hardly addressed, since it is very difficult to say that this low activity is due to the preparation procedure or the low loading, since Co1-MCM-41 with metal content of 1.8 wt.% also gives a low activity. It will be interesting to make some more catalytic

experiments using impregnated Co-MCM-41 with different Co loadings to check this effect.

It is also observed that the conversion increases with temperature. In autoclave, the conversion and efficiency of the  $\text{H}_2\text{O}_2$  are higher compared with those obtained in the glass flask reactor. In the second reaction, the conversion increases compared with that of

Table 2  
Results of the oxidation reactions with  $\text{H}_2\text{O}_2$ <sup>a</sup>

Catalyst	Styrene		Benzene		1-Hexene	
	Conversion (%)	Efficiency <sub>H<sub>2</sub>O<sub>2</sub></sub> (%)	Conversion (%)	Efficiency <sub>H<sub>2</sub>O<sub>2</sub></sub> (%)	Conversion (%)	Efficiency <sub>H<sub>2</sub>O<sub>2</sub></sub> (%)
Fe1-MCM-41	13.8	7.9	10.2	9.4	1.2	18.6
Ni1-MCM-41	6.7	3.3	10.4	6.4	3.5	22.4
Co1-MCM-41	3.1	1.5	1.4	2.8	0.43	12.8
Co-MCM-41(i)	2.4	2.1	1.1	3.4	—	—
Co2-MCM-41	20.2	6.9	66.6	27.1	—	—
Co3-MCM-41	21.1	7.2	67.5	25.4	—	—
Co4-MCM-41	22.3	9.5	75.6	24.5	—	—
Co5-MCM-41	32.7	13.8	80.4	26.1	—	—

<sup>a</sup> Reaction conditions:  $m_{\text{cat}}$ : 70 mg; hydrocarbons/acetonitrile/hydrogen peroxide: 1/3.6/6 for styrene and 1-hexene and 1/—/3 for benzene (reaction without solvent); reaction time and temperature: 2 h at 323 K, glass reactor.

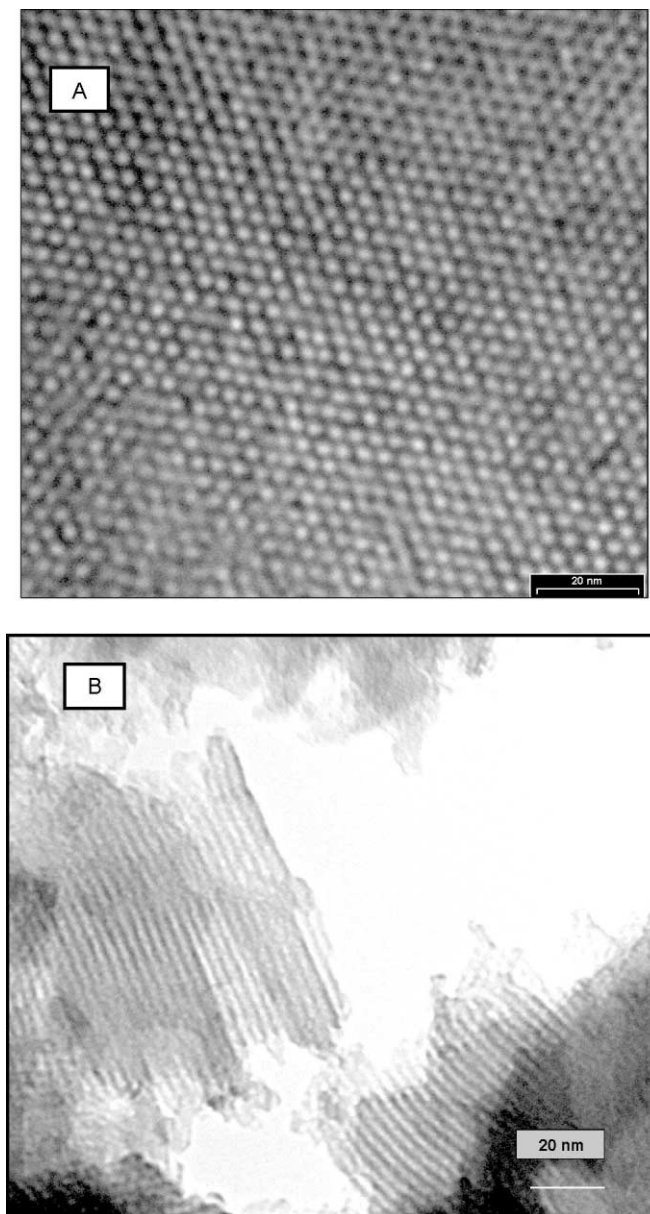


Fig. 4. TEM of Co-MCM-41 material: (A) as-synthesized sample after calcination; (B) after reaction.

the first reaction for the catalysts with a small metal content and decreases for those with higher metal content. A strong adsorption of the aromatic species (benzaldehyde from oxidation of styrene) on the catalyst surface is evidenced by IR spectra (since the complete desorption of adsorbed benzaldehyde species needs an evacuation at 350°C). Leaching of metal ions is

observed for iron-containing catalyst, but is insignificant for the catalysts with a small quantity of cobalt and nickel. The activity of the catalysts is markedly increased when hydrogen peroxide is regularly injected in reaction system in small quantities.

After oxidation reaction, the catalysts conserve their ordered structure (Fig. 4B), indicating no effect of

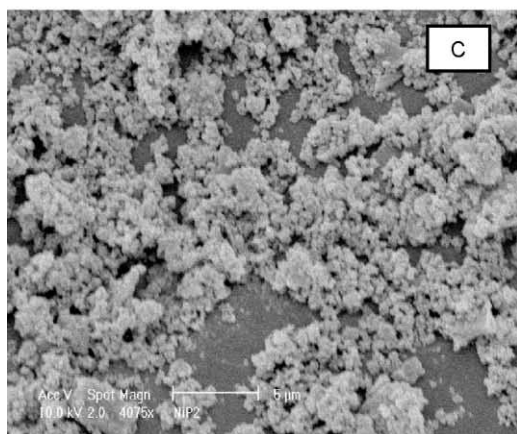
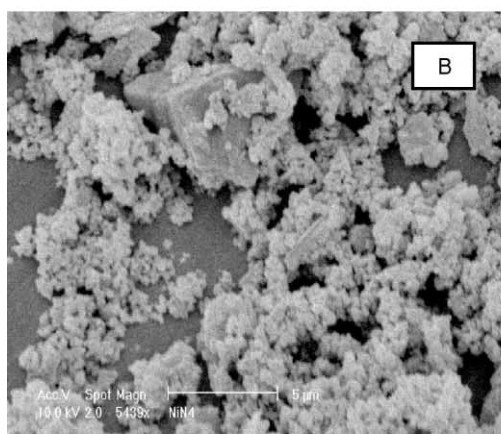
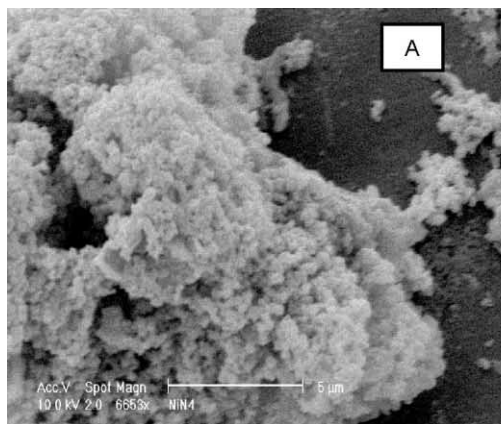


Fig. 5. SEM images of the Ni-MCM-41 catalyst after: calcination (A); first reaction (B); second reaction (C).

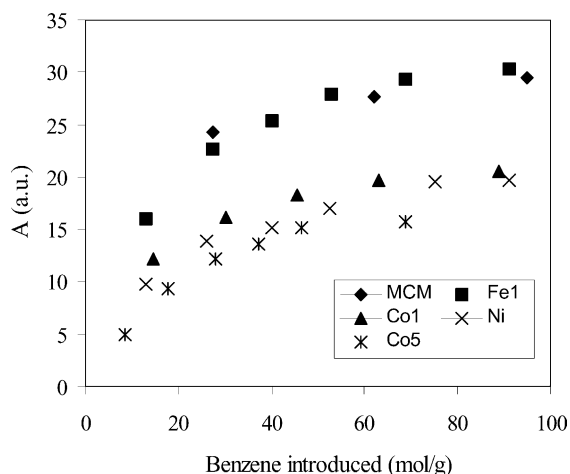


Fig. 6.  $C_6H_6$  adsorption isotherms at 293 K.

reaction on the catalyst structure. Fig. 5B and C show the SEM micrographs of Ni-MCM-41 sample after first cycle reaction (Fig. 5B) and second cycle reaction (Fig. 5C). A morphology of agglomerates of small spheres is still noted; only the size of agglomerates after first and second cycle reaction decreases.

We believe that the incorporation of the iron, cobalt or nickel into an ordered MCM-41 structure affects the chemical state of the metal. The structure and the metal dispersion are responsible for the observed high activity and stability.

#### 4. Conclusions

Mesoporous FeSi-MCM-41, CoSi-MCM-41 and NiSi-MCM-41 materials with a hexagonal and well-ordered structure were synthesized. The metal kind and the metal content incorporated modify the ordered structure and influence the adsorption capacity, activity and stability of the catalysts. Active catalysts were obtained in the oxidation of benzene to phenol and styrene to benzaldehyde.

#### Acknowledgements

This work was performed within the framework of PAI-IUAP 4/10. VP thanks the SSTC (Federal

scientific, technological and cultural office of Premier Minister, Belgium) for a scholarship and a research grant from The University of Namur.

## References

- [1] A. Tuel, *Micropor. Mesopor. Mater.* 27 (1999) 151–167.
- [2] D. Zho, D. Goldfarb, in: L. Bonnevot, S. Kaliaguine (Eds.), *Zeolites: A Refined Tool for Designing Catalytic Sites*, Elsevier, Amsterdam, 1995, pp. 181–188.
- [3] A.J.J. Arnold, J.P.M. Niederer, T.E.W. Nießen, W.F. Hölderich, *Micropor. Mesopor. Mater.* 28 (1999) 353–360.
- [4] M. Hartmann, S. Racouchot, C. Bischof, *Micropor. Mesopor. Mater.* 27 (1999) 309–320.
- [5] S. Suvanto, J. Hukkamäki, T.T. Pakkanen, T.A. Pakkanen, *Langmuir* 16 (2000) 4109–4115.
- [6] M.L.S. Corrêa, M. Wallau, U. Schuchardt, in: H. Chou, S.K. Ihm, Y.S. Uh (Eds.), *Stud. Surf. Sci. Catal.* 105 (1997) 277–283.
- [7] Z. Deng, G.R. Dieckmann, S.H. Langer, *Chem. Commun.* (1997) 1789–1790.
- [8] W.A. Carvalho, M. Wallau, U. Schuchardt, *J. Mol. Catal. A* 144 (1999) 91–99.
- [9] M. Dusi, T. Mallat, A. Baiker, *Catal. Rev.-Sci. Eng.* 42 (2000) 213–278.
- [10] A. Jenty, N.H. Pham, H. Vinek, M. English, J.A. Lercher, *Micropor. Mater.* 6 (1996) 13–17.
- [11] S.-T. Wong, J.F. Lee, S. Cheng, C.-Y. Mou, *Appl. Catal. A* 198 (2000) 115–126.
- [12] N.X. He, S.L. Bao, Q.H. Xu, in: H. Chou, S.K. Ihm, Y.S. Uh (Eds.), *Stud. Surf. Sci. Catal.* 105 (1997) 85–92.
- [13] J.S. Jung, W.S. Chae, R.A. McIntyre, C.T. Seip, J.B. Wiley, C.J. O'Connor, *Mater. Res. Bull.* 34 (1999) 1353–1360.
- [14] J.L. Blin, C. Otjacques, G. Herrier, B.L. Su, *Int. J. Inorg. Mater.* 3 (2001) 75–86.
- [15] B.L. Su, Barthomeuf, *J. Catal.* 139 (1993) 81–92.
- [16] B.L. Su, V. Norberg, *Zeolites* 19 (1997) 65–74.
- [17] B.L. Su, V. Norberg, C. Hansenne, *Langmuir* 16 (2000) 1132–1140.
- [18] B.L. Su, V. Norberg, *Langmuir* 16 (2000) 6020–6028.